

# Primidone inhibits TRPM3 and attenuates thermal nociception in vivo

Ute Krügel<sup>a</sup>, Isabelle Straub<sup>a,b</sup>, Holger Beckmann<sup>a</sup>, Michael Schaefer<sup>a,\*</sup>

## Abstract

The melastatin-related transient receptor potential (TRP) channel TRPM3 is a nonselective cation channel expressed in nociceptive neurons and activated by heat. Because TRPM3-deficient mice show inflammatory thermal hyperalgesia, pharmacological inhibition of TRPM3 may exert antinociceptive properties. Fluorometric  $\text{Ca}^{2+}$  influx assays and a compound library containing approved or clinically tested drugs were used to identify TRPM3 inhibitors. Biophysical properties of channel inhibition were assessed using electrophysiological methods. The nonsteroidal anti-inflammatory drug diclofenac, the tetracyclic antidepressant maprotiline, and the anticonvulsant primidone were identified as highly efficient TRPM3 blockers with half-maximal inhibition at 0.6 to 6  $\mu\text{M}$  and marked specificity for TRPM3. Most prominently, primidone was biologically active to suppress TRPM3 activation by pregnenolone sulfate (PregS) and heat at concentrations markedly lower than plasma concentrations commonly used in antiepileptic therapy. Primidone blocked PregS-induced  $\text{Ca}^{2+}$  influx through TRPM3 by allosteric modulation and reversibly inhibited atypical inwardly rectifying TRPM3 currents induced by coapplication of PregS and clotrimazole. In vivo, analgesic effects of low doses of primidone were demonstrated in mice, applying PregS- and heat-induced pain models, including inflammatory hyperalgesia. Thus, applying the approved drug at concentrations that are lower than those needed to induce anticonvulsive effects offers a shortcut for studying physiological and pathophysiological roles of TRPM3 in vivo.

**Keywords:** Transient receptor potential channel, Melastatin-related, TRPM3, Cation channel, Calcium influx, Patch clamp, Hot plate, Tail flick, Inflammatory hyperalgesia, Clotrimazole

## 1. Introduction

Transient receptor potential (TRP) channels are the second largest family of helix-loop-helix-motif-containing cation channels. They assemble into rotationally symmetric homotetrameric or heterotetrameric complexes to form a central ion-conducting pore.<sup>12,14,18,26</sup> Among others, the third member of the melastatin-related TRPM channel subfamily TRPM3 is expressed in sensory neurons of dorsal root (DRG) and trigeminal ganglia and has recently been shown to contribute to thermal pain perception.<sup>32,33</sup> Like the well-characterized heat-activated vanilloid-related TRPV1, TRPM3 is expressed in small-to-medium diameter DRG neurons, which belong to the group of

heat-sensitive, peptidergic nociceptors that use unmyelinated C-fibres and free nerve endings to sense potentially harmful temperatures in the epidermal–dermal junction.<sup>33</sup>

The TRPM3 gene encodes for numerous different splice variants. Splicing within exon 24 can lead to different TRPM3 proteins that can give rise to a monovalent-selective (TRPM3 <sub>$\alpha$ 1</sub>) or a nonselective (TRPM3 <sub>$\alpha$ 2</sub>) cation conductance.<sup>23</sup> In rodent DRG neurons, the  $\text{Ca}^{2+}$ -permeable TRPM3 <sub>$\alpha$ 2</sub> splice variant is predominantly expressed. TRPM3 <sub>$\alpha$ 2</sub> can be activated by not only warm or hot temperatures but also the neurosteroid pregnenolone sulfate (PregS), high concentrations of nifedipine,<sup>34</sup> or the potent synthetic ligand 3,4-dihydro-*N*-(5-methyl-3-isoxazolyl)- $\alpha$ -phenyl-1(2*H*)-quinolineacetamide (CIM0216).<sup>7</sup> Furthermore, the antifungal drug clotrimazole, in combination with PregS, gives rise to a massive and biophysically distinct sodium ion influx, which has been attributed to an alternative ion permeation pathway of TRPM3, the omega pore.<sup>32</sup>

Upon injection into paws of wild-type mice, PregS induces a transient nociceptive behaviour, which is not observed in TRPM3-deficient mice.<sup>33</sup> In addition, TRPM3 deficiency is associated with a reduction of heat-induced thermal hyperalgesia caused by hind paw injection of complete Freund adjuvant (CFA). By contrast, thermal hypersensitivity to a cold stimulus was maintained, indicating a prominent role of TRPM3 in mediating inflammatory heat hypersensitivity.

In an academic-scale screening endeavour, we have recently identified secondary plant metabolites with a flavanone pharmacophore that potently and selectively inhibit TRPM3.<sup>27,28</sup> These compounds inhibit calcium entry and ionic currents through heterologously expressed TRPM3 <sub>$\alpha$ 2</sub> and blunted TRPM3-like signals in DRG neurons. When applied in vivo, isosakuranetin, the most potent and effective TRPM3-inhibitory flavanone, reduced

Sponsorships or competing interests that may be relevant to content are disclosed at the end of this article.

<sup>a</sup> Rudolf-Boehm-Institut für Pharmakologie und Toxikologie, Universität Leipzig, Leipzig, Germany, <sup>b</sup> Carl-Ludwig-Institut für Physiologie, Universität Leipzig, Leipzig, Germany

\*Corresponding author. Address: Rudolf-Boehm-Institut für Pharmakologie und Toxikologie, Härtelstr. 16-18, 04107 Leipzig, Germany, Tel.: +49 341 9724600; fax: +49 341 9724609. E-mail address: michael.schaefer@medizin.uni-leipzig.de (M. Schaefer).

Supplemental digital content is available for this article. Direct URL citations appear in the printed text and are provided in the HTML and PDF versions of this article on the journal's Web site ([www.painjournalonline.com](http://www.painjournalonline.com)).

PAIN 158 (2017) 856–867

Copyright © 2017 The Author(s). Published by Wolters Kluwer Health, Inc. on behalf of the International Association for the Study of Pain. This is an open-access article distributed under the terms of the Creative Commons Attribution-Non Commercial-No Derivatives License 4.0 (CCBY-NC-ND), where it is permissible to download and share the work provided it is properly cited. The work cannot be changed in any way or used commercially without permission from the journal.

<http://dx.doi.org/10.1097/j.pain.0000000000000846>

heat-induced pain-related behaviour and nocifensive responses in mice that underwent hind paw injection of the TRPM3<sub>α2</sub> activator.<sup>27</sup> Following up on these promising starting points, we also sought to identify biological activities of approved drugs to inhibit TRPM3. By screening a compound library containing Food and Drug Administration (FDA)-approved or clinically tested drugs, we identified the nonsteroidal anti-inflammatory drug diclofenac, the tetracyclic antidepressant maprotiline, and the anticonvulsant primidone as novel TRPM3 blockers. We provide evidence that primidone, a prodrug, which is hepatically metabolized to the active anticonvulsant metabolites phenobarbital and phenylethylmalonamide,<sup>2</sup> effectively and potently inhibits both recombinant and native TRPM3 channel complexes at concentrations much lower than recommended therapeutic plasma values. The concentration dependence, electrophysiological properties, isotype selectivity, and mechanisms of inhibition that contribute to thermal and chemical nociception are characterised. Finally, in vivo experiments corroborated the potential analgesic effect of primidone in PregS- and heat-induced pain and in inflammatory thermal hyperalgesia.

## 2. Materials and methods

### 2.1. Stock solutions and drugs

All modulators were dissolved in dimethyl sulfoxide (DMSO), if not indicated otherwise. Dimethyl sulfoxide concentrations in the final solution never exceeded 0.14% at the highest test concentration of the respective modulator and were further reduced by serial dilution of the compounds. Pregnenolone sulfate, allyl isothiocyanate (AITC), CFA (containing 1 mg·mL<sup>-1</sup> of heat-killed and dried mycobacterium), diclofenac, maprotiline, primidone, and clotrimazole were purchased from Sigma-Aldrich (Deisenhofen, Germany). For behavioural studies, primidone was suspended in 0.5% Tween 20 (Sigma-Aldrich) which was also used as vehicle control.

### 2.2. Cell culture

Human embryonic kidney (HEK293) cells stably expressing myc-tagged mouse TRPM3<sub>α2</sub> (HEK<sub>mTRPM3</sub>) were obtained and maintained as described earlier.<sup>28</sup> HEK293 cells stably expressing rat TRPV1 (HEK<sub>rTRPV1</sub>), human TRPM8 (HEK<sub>hTRPM8</sub>), or human ankyrin-like TRPA1 (HEK<sub>hTRPA1</sub>) were obtained by a limiting dilution method as described earlier.<sup>8,31</sup> Parental HEK293 cells served as controls. All cells were grown at 37°C in a humidified atmosphere containing 5% CO<sub>2</sub>. Unless otherwise stated, cells were seeded 24 hours prior to the experiments onto poly-L-lysine-coated coverslips.

For transient transfection with human TRPM3, HEK293 cells were grown in minimal essential medium supplemented with Earle's salts (Biochrom GmbH, Berlin, Germany), with 10% foetal calf serum (Invitrogen, Carlsbad, CA), 2 mM L-glutamine (Biochrom), 100 U·mL<sup>-1</sup> penicillin (Biochrom), and 100 μg·mL<sup>-1</sup> streptomycin (Biochrom). One to 2 days after seeding, cells were transfected with 2 μg of plasmid DNA encoding a TRPM3 C-terminally fused to yellow fluorescent protein using Fugene HD transfection reagent (Roche Diagnostic, Mannheim, Germany). Two days after transfection, cells were used for experiments. DRG neurons were isolated from 8-week-old male and female Wistar rats (Janvier, Le Genest-Saint-Isle, France) as described previously.<sup>28</sup>

### 2.3. Intracellular Ca<sup>2+</sup> analysis in cell suspensions

All fluorometric assays in cell suspensions were performed in 384-well plates as described elsewhere.<sup>22,28</sup> Shortly, HEK293

cells stably expressing TRPM3 were incubated with Fluo-4/AM (4 μM; Life Technologies, Eugene, OR) for 30 minutes at 37°C, washed and resuspended in 10 mM HEPES-buffered solution (HBS) buffer, containing 135 mM NaCl, 6 mM KCl, 1 mM CaCl<sub>2</sub>, 1 mM MgCl<sub>2</sub>, 5.5 mM D-glucose, and 10 mM HEPES, and adjusted to pH 7.4 with NaOH. For the primary screening, wells were pre-filled with individual compounds of the Spectrum Collection compound library (MicroSource Discovery Systems, Gaylordsville, CT) and prediluted in HBS to reach a final concentration of 20 μM after adding the Fluo-4-loaded cell suspension. Fluorescence was monitored with a filter-based plate reader device (POLARstar Omega, BMG Labtech, Offenburg, Germany) in the bottom-read mode, applying 485/10 nm and 520/20 nm band pass filters for excitation and emission, respectively, or using a custom-made fluorescence plate imaging device built into a robotic liquid handling station (Freedom EVO 150; Tecan Group, Männedorf, Switzerland), as recently described.<sup>22</sup> Pregnenolone sulfate (35 μM or as otherwise indicated) was added to each well after recording the baseline for 160 seconds, and fluorescence intensities were followed for further 600 seconds. To correct for unequal loading and detection sensitivity, background signal-corrected fluorescence intensities (F) measured in single wells were normalized to the respective initial intensities (F<sub>0</sub>). To obtain the IC<sub>50</sub> with SEM and Hill coefficients, data from different concentrations of TRPM3 modulators were plotted using OriginPro 8.0 (OriginLab, Northampton, MA) and fitted, applying a 4-parameter Hill equation to obtain minimum and maximum effect levels, the IC<sub>50</sub> values, and Hill coefficients.

To test the selectivity of diclofenac, maprotiline, and primidone similar experiments were performed with HEK<sub>hTRPA1</sub>, HEK<sub>rTRPV1</sub>, and HEK<sub>hTRPM8</sub>. TRPV1-, TRPM8-, and TRPA1-expressing HEK cells were stimulated with capsaicin (2 μM), menthol (300 μM), and AITC (30 μM), respectively.

### 2.4. Single-cell measurement of intracellular Ca<sup>2+</sup> concentration [Ca<sup>2+</sup>]<sub>i</sub> and heat-induced TRPM3 activation

Fura-2/AM-loaded (5 μM; Biotium, Hayward, CA) HEK<sub>mTRPM3</sub> cells and rat DRG neurons attached to poly-L-lysine-coated coverslips were subjected to single-cell measurement of [Ca<sup>2+</sup>]<sub>i</sub> as previously described.<sup>28</sup> The fluorescence was alternately assessed at excitation wavelengths of 340 and 380 nm. The ratio of the respective background-corrected fluorescence intensities (F<sub>340</sub>/F<sub>380</sub>) was calculated and depicted. All measurements were performed at room temperature (22–24°C). For heat activation experiments, HEK<sub>mTRPM3</sub> cells were perfused with HBS heated to ~37°C with an in-line heater device (TC-324C; Warner Instruments, Hamden, CT). The actual temperature was monitored with a thermistor electrode situated next to the recorded cells.

### 2.5. Whole-cell patch-clamp measurements

All electrophysiological measurements were taken in the voltage-clamped whole-cell mode at room temperature as previously described,<sup>27</sup> using an Axopatch 200B amplifier connected to a desktop computer by a Digidata 1200 digitizer (Axon CNS; Molecular Devices, Sunnyvale, CA) under the control of pCLAMP10 software (Molecular Devices). To obtain current density-voltage curves, holding potential (V<sub>h</sub>) was set to -113 mV for 100 milliseconds and voltage ramps from -113 to +87 mV (0.4 mV ms<sup>-1</sup>) were applied in 1-second intervals. Voltage ramps in experiments with omega-pore activation by combined stimulation with PregS and clotrimazole ranged from -126 to

+74 mV to monitor the inward rectification. The liquid junction potential between bath and pipette solutions was 13 mV (calculated with Clampex, Molecular Devices) and corrected for. The intersweep holding potential was  $-13$  mV. The intracellular solution contained 80 mM Cs-aspartate, 45 mM CsCl, 4 mM  $\text{Na}_2\text{ATP}$ , 10 mM 1,2-bis(o-aminophenoxy)ethane-N,N,N',N'-tetraacetic acid (BAPTA), and 5 mM EGTA, and 10 mM HEPES adjusted to pH 7.2 with CsOH. The osmolarity was 300 to 315 mOsm. The extracellular solution contained 145 mM NaCl, 3 mM KCl, 10 mM CsCl, 2 mM  $\text{CaCl}_2$ , 2 mM  $\text{MgCl}_2$ , 10 mM D-glucose, and 10 mM HEPES at pH 7.4, adjusted with NaOH. Series resistance was  $<10$  M $\Omega$  and compensated by 75% to 85%. Data were filtered with a low-pass Bessel filter at 10 kHz. The sampling rate was 5 kHz in standard whole-cell measurements. Modulators were locally applied through a triple barrel glass tube positioned in close proximity to the patched cell and controlled with a SF-77B Perfusion Fast Step system (Warner Instruments, Hamden, CT).

## 2.6. Animals and behavioural analysis

All experiments were conducted in strict accordance with the accepted standards of animal care (European Communities Council; Directive 2010/63/EU, Guide for the Care and Use of Laboratory Animals; NIH<sup>21</sup>) and were approved by the government of the State of Saxony (Ethics Committee, Landesdirektion Sachsen, Leipzig, Germany; permission number TWV 02/12). Studies involving animals are reported in accordance with the ARRIVE guidelines for reporting experiments involving animals.<sup>10,16</sup>

Ten- to 12-week-old male C57BL/6J mice (25–30 g; Charles River Laboratories, Sulzfeld, Germany) were housed in groups of 4 to 5 earmarked mice per cage under standard conditions (12 h: 12 h light–dark cycle, lights on at 7 AM, 22°C, 60% relative humidity) with free access to standard laboratory chow and water. All experiments were performed between 8:00 and 12:00 AM. Mice were randomized within the cages for the different experimental groups and used only once. The group size (n) refers to independent values in each experimental group and is provided in the figure legends. All behavioural observations were made blind to treatments which were performed by another operator.

## 2.7. Behavioural tests

Pregnenolone sulfate–induced chemical pain was assessed immediately after intraplantar injection (i.pl.) of 5 nmol PregS into the right hind paw either in a mixture with 10 nmol primidone or vehicle or 5 minutes after local pretreatment with primidone. A total volume of 10  $\mu\text{L}$  was applied to each paw. Pregnenolone sulfate was dissolved in sterile water and primidone was suspended in 0.5% Tween 20. Furthermore, responses to PregS-induced pain were registered 20 minutes after intraperitoneal (i.p.) administration of primidone at doses of 0.5, 2, and 10  $\text{mg}\cdot\text{kg}^{-1}$  of body weight. The latency to the first response after injection (licking, lifting, and shaking) and the total duration of responses were recorded up to 180 seconds.<sup>27,33</sup>

To examine dose effects of systemically administered primidone (0.5, 2, and 10  $\text{mg}\cdot\text{kg}^{-1}$ , i.p.) on thermal nociception, mice were placed on a thermostated (52°C) hot plate (Ugo Basile, Geminio, Italy) 20 minutes after primidone injection. The latency to the first nocifensive hind paw response was registered. The animals were removed from the apparatus immediately thereafter or at latest after a cutoff time of 45 seconds. To evaluate potential interference of gross behavioural activity with pain responses

induced by systemic primidone and its metabolites, the exploratory motor activity was monitored for 5 minutes immediately before the hot plate test and again 120 minutes after drug administration. The travelled distance in an opaque plastic box (50  $\times$  50  $\times$  40 cm) was evaluated using a computer-assisted video activity measurement system (VideoMot; TSE, Bad Homburg, Germany). Primidone effects (1  $\text{mg}\cdot\text{kg}^{-1}$ , i.p.) on thermal nociception were additionally verified in the tail immersion test. Mice were placed in a 50 mL polypropylene conical tube. The distal half of the protruding tail was dipped into hot water controlled at  $48.0 \pm 0.5^\circ\text{C}$ . Latency to the vigorous flexion of the tail in response to the heat stimulus was registered and a cutoff time set at 15 seconds.

To prove analgesic effects of primidone on thermal hyperalgesia evoked by inflammation, 20  $\mu\text{L}$  CFA or sterile saline (controls) were injected into both hind paws subsequent to measurement of original hind paw thickness. Twenty-four hours later, paw thickness was measured again, followed by systemic administration of primidone (1  $\text{mg}\cdot\text{kg}^{-1}$ ) or vehicle 20 minutes before the hot plate test. The latency to hind paw responses was registered and the trial terminated as in the hot plate test.

## 2.8. Statistical analysis

All data are expressed as mean  $\pm$  SEM. The number of cells or animals analysed in each experiment is indicated in the figure legends. In vitro data were analysed with OriginPro 8G (OriginLab) and behavioural results were analysed using the statistic tool of SigmaPlot (Version 11.0; Systat Software, Inc, San Jose, CA). To test for statistically significant differences in the patch-clamp measurements and behavioural experiments with intraperitoneal administration of primidone, one-way analysis of variance was used. Primidone effects on heat-induced  $\text{Ca}^{2+}$  influx and on clotrimazole-enhanced currents were analysed using analysis of variance with repeated measurements. Tukey post hoc followed all analyses. Effects of intraplantarly administered primidone on the PregS-induced nociception and the CFA-induced paw swelling were proofed using the 2-tailed unpaired Student *t* test. The threshold for statistical significance was defined at  $P < 0.05$  consistently. Complete values of statistical analysis are given in supplemental digital content (SDC; Table S1, available online at <http://links.lww.com/PAIN/A386>).

## 3. Results

### 3.1. Identification of TRPM3-inhibiting approved drugs

To identify approved or clinically tested drugs that modulate TRPM3 activity, we screened a library of 800 drugs with respect to a possible biological activity to inhibit  $\text{Ca}^{2+}$  entry through TRPM3. To this end, Fluo-4-loaded suspensions of stably transfected HEK<sub>mTRPM3</sub> cells were incubated with the drugs diluted to a final concentration of 20  $\mu\text{M}$  in single wells of 384-well plates. After baseline recording for 2 minutes, the TRPM3 activator PregS (35  $\mu\text{M}$ ) was applied, and  $\text{Ca}^{2+}$  responses were followed for another 10 to 15 minutes. Within this primary screen, we annotated and validated 4 approved drugs that completely blocked PregS-induced  $\text{Ca}^{2+}$  entry at the applied test concentration.

Mefenamic acid was reidentified, whereas the related fenamates, flufenamic acid, and tolfenamic acid were less potent and poorly specific TRPM3 inhibitors (data not shown<sup>11</sup>). Furthermore, the nonsteroidal anti-inflammatory drug diclofenac, the tetracyclic antidepressant maprotiline, and the anticonvulsant barbiturate precursor drug primidone were identified (Fig. 1). Apart from diclofenac,

these have not previously been known to inhibit  $Ca^{2+}$  entry through TRPM3.<sup>29</sup> Because the data appeared as high-quality data with no discernible interference, which might result eg, from fluorescence, absorbance, or toxic effects of the compounds, results were followed up in more detail, applying the same  $Ca^{2+}$  assay.

### 3.2. Concentration dependence of drug-induced inhibition of TRPM3-dependent $Ca^{2+}$ entry and ionic currents

To assess the potency of TRPM3 inhibition by diclofenac, maprotiline, and primidone, Fluo-4-loaded HEK<sub>mTRPM3</sub> cells were exposed to various concentrations of the respective drugs, and the PregS-induced  $Ca^{2+}$  signal was measured to construct concentration response curves and to obtain an estimate of the half maximal inhibitory concentrations ( $IC_{50}$ ). All 3 compounds inhibited TRPM3-mediated  $Ca^{2+}$  entry in a concentration-dependent fashion (Fig. 2).

During preparation of this work, Suzuki et al.<sup>29</sup> reported that diclofenac is an antagonist for human TRPM3 isoforms.

Corroborating their data, diclofenac displayed the lowest potency as a TRPM3 blocker with an  $IC_{50}$  of  $6.2 \pm 0.4 \mu M$  (Fig. 2A). Maprotiline blocked TRPM3 responses with an  $IC_{50}$  of  $1.3 \pm 0.13 \mu M$ , and primidone was the most potent TRPM3-inhibiting drug, with an  $IC_{50}$  of  $0.6 \pm 0.15 \mu M$  (Fig. 2B, C). The Hill coefficients of all 3 drugs indicated only a limited cooperativity in suppressing the channel function, diclofenac:  $1.2 \pm 0.1$ , maprotiline:  $1.3 \pm 0.1$ , and primidone:  $1.4 \pm 0.2$ .

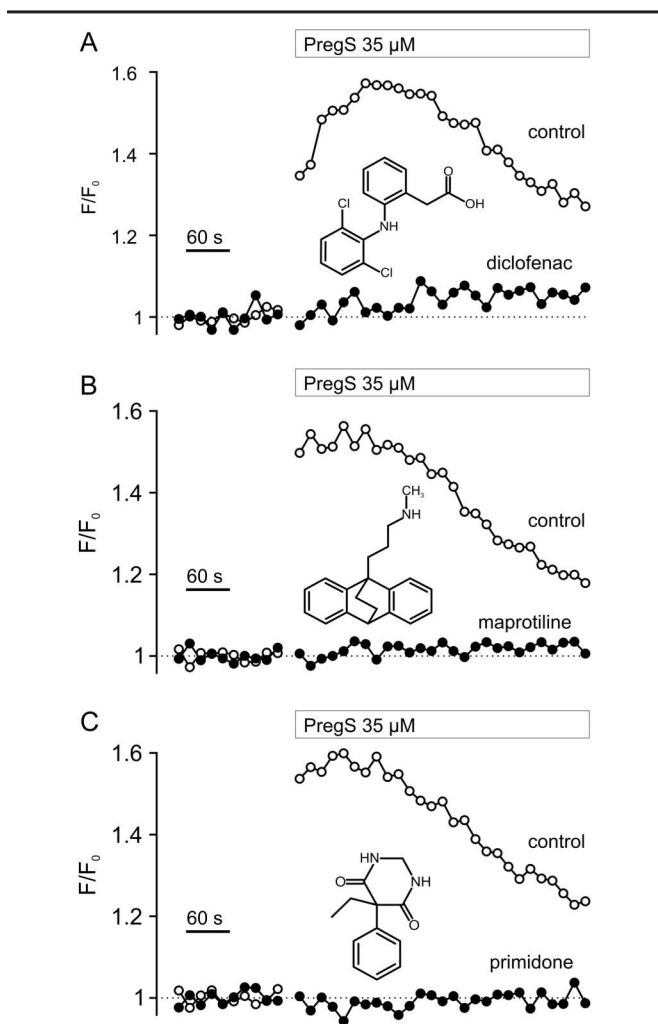


**Figure 1.** Identification of diclofenac (A), maprotiline (B), and primidone (C) as inhibitors of TRPM3. Fluo-4-loaded HEK<sub>mTRPM3</sub> cells were incubated with 20 μM of single compounds (black circles) or with 0.2% DMSO concentration (control, white circles), and fluorescence intensities were measured during injection of 35 μM pregnenolone sulfate as indicated by the bars. Fluo-4 fluorescence intensities F were normalised to the respective initial intensities F<sub>0</sub> and depicted as time course. Traces extracted from the original screening data set, performed in a 384-well plate format, are shown along with the chemical structures of the respective drugs.

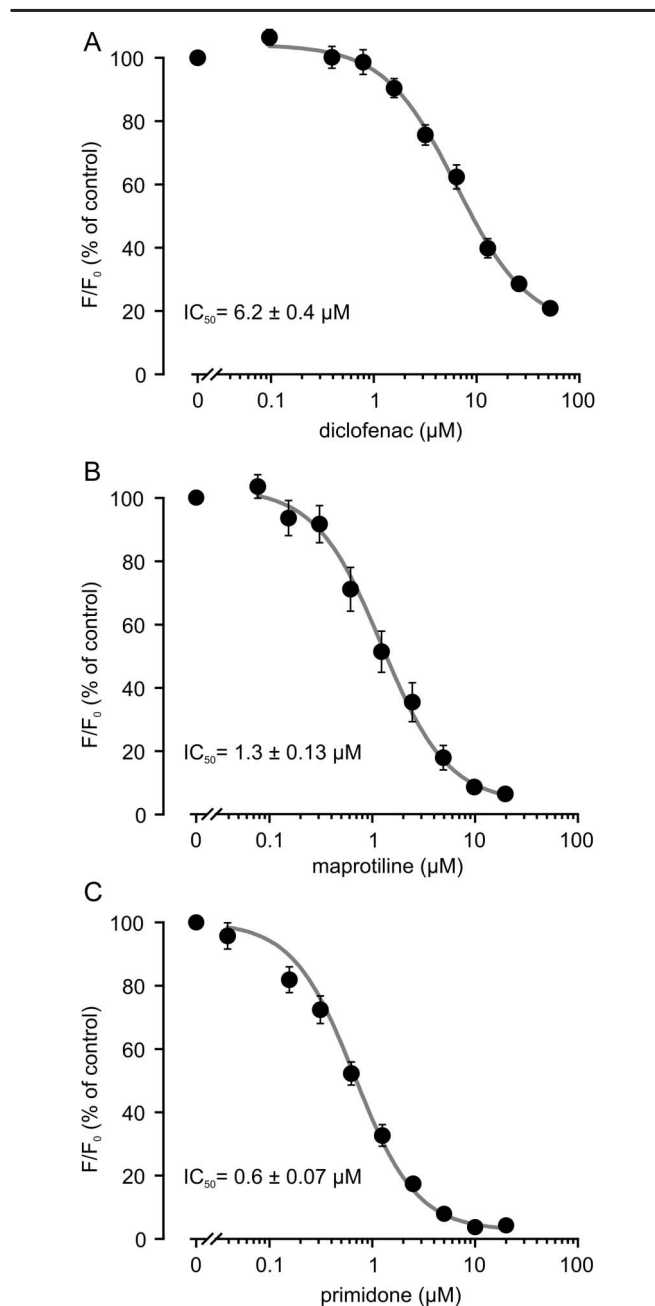


**Figure 2.** Concentration-dependent inhibition of pregnenolone sulfate-induced  $Ca^{2+}$  entry through TRPM3. Concentration–response curves for diclofenac (n = 9) (A), maprotiline (n = 8) (B), and primidone (n = 8) (C) were obtained by incubating HEK<sub>mTRPM3</sub> cells with various concentrations of the respective drug and measuring the pregnenolone sulfate-induced activation of TRPM3. Activation without an inhibitor (DMSO control) was set as 100%, and fluorescence intensities evoked by solutions containing inhibitors were normalized to this value.  $IC_{50}$  values were obtained by fitting a 4-parameter Hill equation to each experiment, and mean values and SEM were calculated as shown.

Because Fluo-4 fluorescence intensities indicate steady-state  $\text{Ca}^{2+}$  concentrations and do not scale with  $[\text{Ca}^{2+}]_i$  in a linear fashion, a more direct and quantitative characterisation of TRPM3 inhibition was achieved using electrophysiological patch-clamp measurements of TRPM3 currents in the whole-cell configuration. Pregnenolone sulfate-induced TRPM3 currents were measured in HEK<sub>mTRPM3</sub> cells, and drugs were acutely added to the bath solution at different test concentrations in the continued presence of PregS.

In agreement with Suzuki et al.,<sup>29</sup> the onset of the diclofenac-induced TRPM3 block was fast, and TRPM3 current inhibition was reversible (SDC Fig. S1). At 25  $\mu\text{M}$ , diclofenac almost completely abolished PregS-induced inward and outward currents with no overt signs of a voltage-dependent mode of action and without changing the reversal potential (SDC Fig. S1A–C). At a concentration of 5  $\mu\text{M}$ , diclofenac caused an inhibition of the physiologically relevant, depolarizing inward currents by about 70% (SDC Fig. S1C).

Maprotiline showed similar effects, although the washout of the drug was associated with a more delayed recovery of ionic currents (Fig. 3). A test concentration of 1.25  $\mu\text{M}$  caused about 75% inhibition of inward currents, again arguing for a slight underestimation of the potency with the fluorometric  $\text{Ca}^{2+}$  assay. Like diclofenac, maprotiline was effectively inhibiting both inward and outward currents with no significant shifts in the reversal potential.

With a pKa value of 4.15, the predominant (>99%) micro-species of diclofenac at physiological pH is deprotonized and, thus, negatively charged. Therefore, its permeation through

biological membranes may be restricted, possibly allowing a differentiation between an intracellularly or extracellularly located binding site. To explore these possibilities, we performed whole-cell measurements with diclofenac-containing pipette solutions. Intracellularly perfused diclofenac (25  $\mu\text{M}$ ) did not prevent PregS-induced currents. Instead, PregS-induced TRPM3 currents had similar current densities compared with those measured in HEK<sub>mTRPM3</sub> cells that were patched with standard pipette solution (compare SDC Fig. S1F and S1C). In HEK<sub>mTRPM3</sub> cells that displayed TRPM3 currents despite intracellular perfusion with diclofenac, the additional exposure to diclofenac from the extracellular side was still effectively inhibiting TRPM3 currents in the same cells (SDC Fig. S1D–F). These data hint to an extracellular accessibility of the binding site for diclofenac. At neutral pH, the major micro-species of the basic drug maprotiline is the protonated, cationic form. Intracellular perfusion with maprotiline via the pipette solution again failed to prevent PregS-induced TRPM3 currents, while addition of maprotiline via the bath solution remained effective (Fig. 3D–F). Considering the highly lipophilic core structure of maprotiline and the slow current recovery after omission of the drug from the bath solution, we cannot conclude about the location of its binding site from our experimental data.

For primidone, a submicromolar potency to block TRPM3 currents was confirmed by electrophysiological recordings, and PregS-induced inward currents were almost completely abolished by 3 and 5  $\mu\text{M}$  primidone (Fig. 4). Again, TRPM3 current inhibition was reversible, repeatable, and displayed no marked voltage dependence of the block. Because primidone is

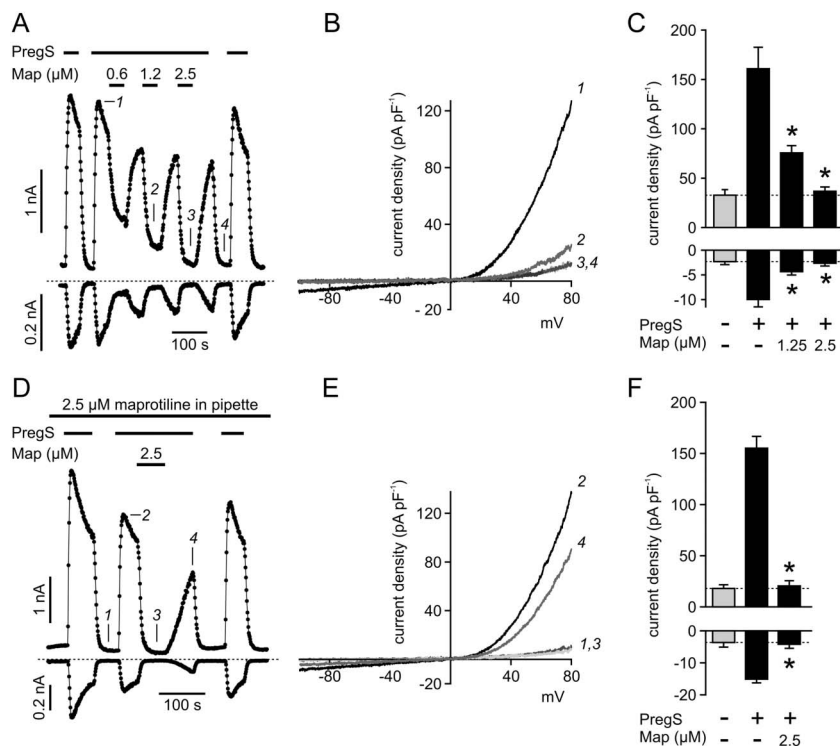


**Figure 3.** Electrophysiological characterisation of the maprotiline-induced TRPM3 inhibition. (A) Representative whole-cell currents from a HEK<sub>mTRPM3</sub> cell after alternating application of 35  $\mu\text{M}$  of pregnenolone sulfate (PregS) and different concentrations of maprotiline (Map). Data are extracted from voltage ramps and depict currents at 87 mV (upper trace) and  $-113$  mV (lower trace). The zero current level is indicated as dotted line. (B) Current density–voltage relation for PregS-induced TRPM3 currents at time points as indicated in (A) before (1), during (2), and after (3, 4) application of different concentrations of maprotiline ( $\mu\text{M}$ ). (C) Statistical analysis of peak current densities ( $n = 12$  for control and pregnenolone sulfate;  $n = 13$  for PregS plus maprotiline) performed as in (A). Background conductivity is shown as dotted line. (D–F) Similar measurement as performed in (A–C) but activation and inhibition of PregS-induced currents were performed in the presence of 2.5  $\mu\text{M}$  of maprotiline in the pipette solution ( $n = 4$  each). Data are presented as mean values  $\pm$  SEM. \* $P < 0.05$  vs PregS alone.

expected to be uncharged at physiological pH, a restriction to either side of the plasma membrane is unlikely, and we did not test the effects of the intracellularly perfused drug. Besides PregS- or heat-induced activation of outwardly rectifying TRPM3 currents, costimulation with PregS and clotrimazole has been described to induce large, inwardly rectifying currents.<sup>32</sup> On performing whole-cell patch-clamp experiments with HEK<sub>m</sub>TRPM3 cells, we confirmed this observation (Fig. 4D–F). Primidone (10 μM) also inhibited the omega pore-like currents evoked by coapplied PregS and clotrimazole.

**3.3. Selectivity of TRPM3 inhibition by diclofenac, maprotiline, and primidone**

The selectivity of TRPM3 inhibition was tested in stably transfected HEK293 cell lines, expressing either the thermosensitive TRPV1, the cold and menthol receptor TRPM8, or the irritant-sensing TRPA1. None of the 3 drugs had an inhibitory effect on capsaicin-induced TRPV1 activation (Fig. 5A–C). Diclofenac attenuated responses to AITC stimulation in HEK<sub>h</sub>TRPA1 cells by about 50% when applied at concentrations higher than 50 μM (Fig. 5A). Because diclofenac is known to activate TRPA1 at high concentrations (EC<sub>50</sub> = 210 μM), the apparent inhibition of AITC-induced calcium entry in TRPA1 expressing cells mimicked a previous activation of TRPA1 during the incubation.<sup>9</sup> The activation of HEK<sub>h</sub>TRPM8 cells was almost unaffected by diclofenac.

The selectivity profile of maprotiline and primidone was the most promising one, with no apparent inhibition of the respective channel at concentrations up to 50 μM (Fig. 5B,C). Other TRP

channels, such as human TRPM2, the canonical mouse TRPC5, and human TRPC6, or human P2X7 receptors were not discernibly inhibited by either of the 3 drugs (tested at a final concentration of 20 μM) with the exception that diclofenac at concentrations above 1 μM caused a partial inhibition of H<sub>2</sub>O<sub>2</sub>-induced [Ca<sup>2+</sup>]<sub>i</sub> signals in HEK cells expressing human TRPM2 (data not shown). Because reported therapeutic plasma concentrations of diclofenac and maprotiline are markedly lower than those that are required to efficiently block TRPM3 in vitro, we focused on primidone, whose therapeutic plasma concentrations reach 20 to 50 μM.<sup>20</sup>

**3.4. Primidone acts as an inhibitory allosteric modulator and suppresses TRPM3-dependent Ca<sup>2+</sup> entry induced by thermal stimulation**

To test whether inhibition of TRPM3 by primidone is surmountable by high activator concentrations, we applied FLIPR analyses to HEK<sub>m</sub>TRPM3 cells, incubated in the presence of various primidone concentrations, and then stimulated with a variety of PregS concentrations (Fig. 6A). Without primidone, saturating PregS concentrations were reached at about 50 μM. After exposure to 1 to 10 μM primidone, the EC<sub>50</sub> of PregS was increased. More prominently, however, the maximum effect level of 50 to 400 μM PregS was strongly decreased, and remaining activation was characterised by a lower cooperativity (Table 1). The nonsurmountable inhibition either argues for a noncompetitive, allosteric mode of action or may indicate a competitive, irreversible binding mode. Because the latter can be excluded

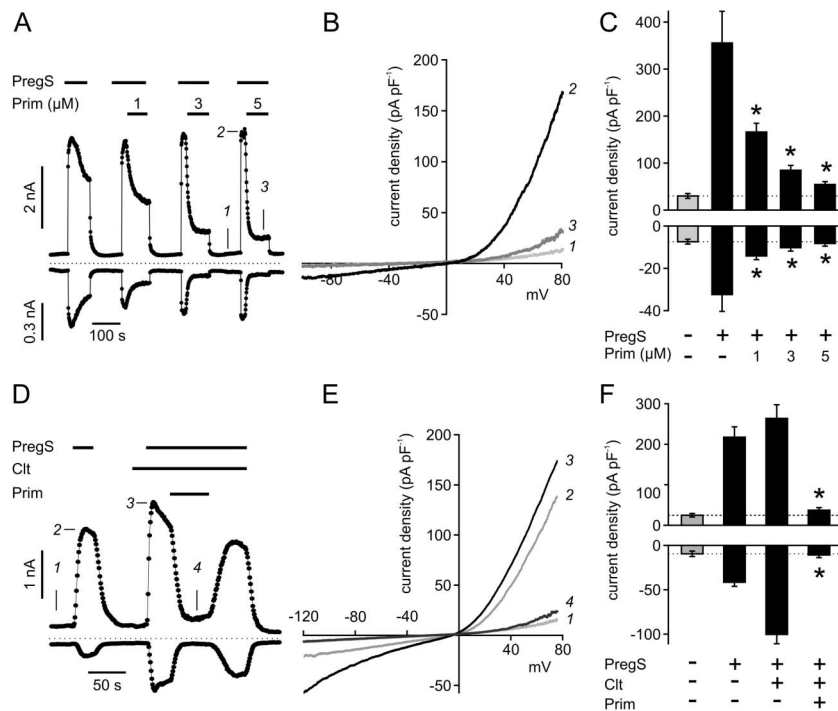


**Figure 4.** Pregnenolone sulfate (PregS)-induced currents are potently and reversibly inhibited by primidone in HEK<sub>m</sub>TRPM3 cells. (A) Whole-cell currents were stimulated with 35 μM PregS, and different concentrations of primidone (Prim) were added as illustrated by the horizontal bars. Data show currents at 87 mV (upper trace) and -113 mV (lower trace). Zero current level is indicated as dotted line. (B) Current density–voltage relation for basal (1), PregS-induced (2), and primidone-blocked current (3) at time points indicated in (A). (C) Statistical analysis of peak current densities performed as in (A) (n = 5 for PregS plus primidone 5 μM, all others n = 7). Dotted line: level of background conductivity. (D) Whole-cell currents were stimulated with 40 μM PregS and 10 μM clotrimazole (Clt). Primidone (10 μM) was added as indicated by the horizontal bars. Data show currents at 74 mV (upper trace) and -126 mV (lower trace). (E) Current density–voltage relation for basal (1), PregS-induced (2), clotrimazole plus PregS-induced (3), and primidone-blocked current (4) at time points indicated in (D). (F) Statistical analysis of peak current densities determined as shown in (D) (n = 6). Data are presented as mean values ± SEM. \*P < 0.05 vs PregS alone or PregS + Clt.

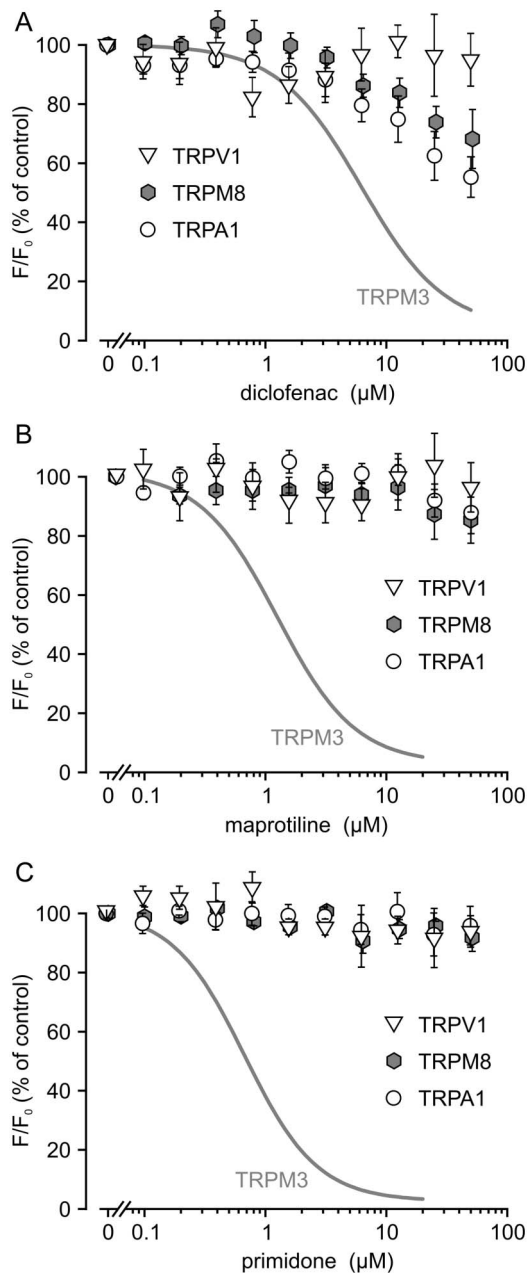


**Figure 5.** Selectivity of TRPM3 inhibition by diclofenac, maprotiline, and primidone in comparison with other nociceptive TRP channels.  $[\text{Ca}^{2+}]_i$  signals in stably TRPV1-, TRPM8-, and TRPA1-expressing HEK293 cell lines were evoked by capsaicin (2  $\mu\text{M}$ ), menthol (300  $\mu\text{M}$ ), and AITC (30  $\mu\text{M}$ ), respectively. The TRPM3-inhibiting drugs diclofenac (A), maprotiline (B), or primidone (C) were applied at different concentrations up to 50  $\mu\text{M}$ . Data are presented as mean values  $\pm$  SEM of 4 independent measurements performed in duplicates each. For comparison of selectivity of drugs for TRPM3, the respective nonlinear fits from Figure 2 are replotted as gray lines.

based on the observed reversibility of TRPM3 current inhibition (Fig. 4A, D), we conclude that primidone presumably binds to a site distinct from the PregS binding site.

Similar to what was previously shown by Vriens et al.,<sup>33</sup> TRPM3-expressing cells responded to a rapid increase in temperature from 22 to 37°C with robust  $[\text{Ca}^{2+}]_i$  signals (Fig. 6B, C). In Fura-2-loaded HEK<sub>mTRPM3</sub> cells, the acute application of primidone (10  $\mu\text{M}$ ) during heat-induced TRPM3 activation led to a rapid and reversible decrease in  $[\text{Ca}^{2+}]_i$ . Application of a second heat stimulus resulted in partly desensitized responses,

but the inhibition by primidone was preserved. Minor apparent  $[\text{Ca}^{2+}]_i$  increases in heat-stimulated parental HEK cells were unaffected by primidone and are most likely caused by temperature-dependent changes of  $\text{Ca}^{2+}$  binding and fluorescence properties of the dye.<sup>3,24</sup>

### 3.5. Primidone blocks calcium signals in isolated rat dorsal root ganglia neurones and human TRPM3

To test the efficiency of primidone to suppress TRPM3-like responses in small-to-medium diameter DRG neurones, lumbar DRG were explanted from adult rats. These DRG neuron subpopulations contain nociceptive neurones that have been reported to express TRPM3.<sup>33</sup> In line with previous findings in our group,<sup>28</sup> about 60% to 70% of these neurones showed a PregS-induced increase in  $[\text{Ca}^{2+}]_i$ , as determined by microfluorometric single-cell analyses in Fura-2-loaded rat DRG neurones (Fig. 7A). In almost all PregS-responsive DRG neurones, the addition of 10  $\mu\text{M}$  primidone caused an immediate decrease in  $[\text{Ca}^{2+}]_i$ , indicating an inhibition of native, TRPM3-bearing channel complexes. Notably, most PregS-sensitive neurones also responded to a challenge with 2  $\mu\text{M}$  capsaicin, supporting the notion of a marked overlap of TRPM3 and TRPV1 expression in heat-sensitive nociceptive neurones (Fig. 7A).  $[\text{Ca}^{2+}]_i$  responses of capsaicin treatment were not discernibly inhibited by 10  $\mu\text{M}$  primidone (data not shown). Qualitative functional studies measuring  $[\text{Ca}^{2+}]_i$  in transiently transfected HEK293 cells expressing the human TRPM3 <sub>$\alpha$ 2</sub> confirmed the effectiveness of primidone on PregS-induced responses at the human TRPM3 channel (Fig. 7B).

### 3.6. Primidone attenuates the sensitivity of mice to chemical and thermal stimulation

Consequently to the in vitro results, the effectivity of primidone to inhibit TRPM3-mediated chemical and thermal nociception was investigated in vivo. The endogenous neurosteroid and TRPM3-activator PregS has been shown to elicit pain when administrated into the hind paw of mice, a response that was lacking in TRPM3-deficient mice.<sup>27,30,33</sup> Systemically applied primidone is metabolized to sedative barbiturate compounds.<sup>13,17</sup> Because, in addition, the evolved phenobarbital can induce hyperalgesia,<sup>34</sup> we preferred first to prove analgesic effects on PregS-induced pain by local injection of primidone into the hind paw. As the local biodistribution and kinetics of TRPM3 occupation by PregS and primidone in vivo is not known, both compounds were either coinjected as a mixture or, to ascertain a preoccupation of TRPM3 with the inhibitor, primidone was injected 5 minutes prior to PregS. The latency to and duration of nocifensive events after blocking TRPM3 by primidone (10 nmol) were registered at a PregS dose of 5 nmol. In both application schemes (coinjection and sequential injection), primidone-treated animals exerted significantly attenuated nocifensive responses to chemical pain induced by TRPM3 activation by PregS (Fig. 8A, B).

Having provided first evidence for local antinociceptive effects of primidone, we applied increasing doses of primidone intraperitoneally, which are reported to yield plasma concentrations beginning from slightly beyond the  $\text{IC}_{50}$  determined in vitro.<sup>13</sup> In response to PregS-induced pain, primidone had a biphasic dose–response effect on latency and total response duration (Fig. 8C, E), with significant antinociception at 0.5  $\text{mg}\cdot\text{kg}^{-1}$ . The number of responses was not altered (Fig. 8B). Planned analysis in addition revealed that nociception was significantly reduced or intensified compared with controls by pretreatment with 0.5 or 10  $\text{mg}\cdot\text{kg}^{-1}$  primidone, respectively, when recalculating the

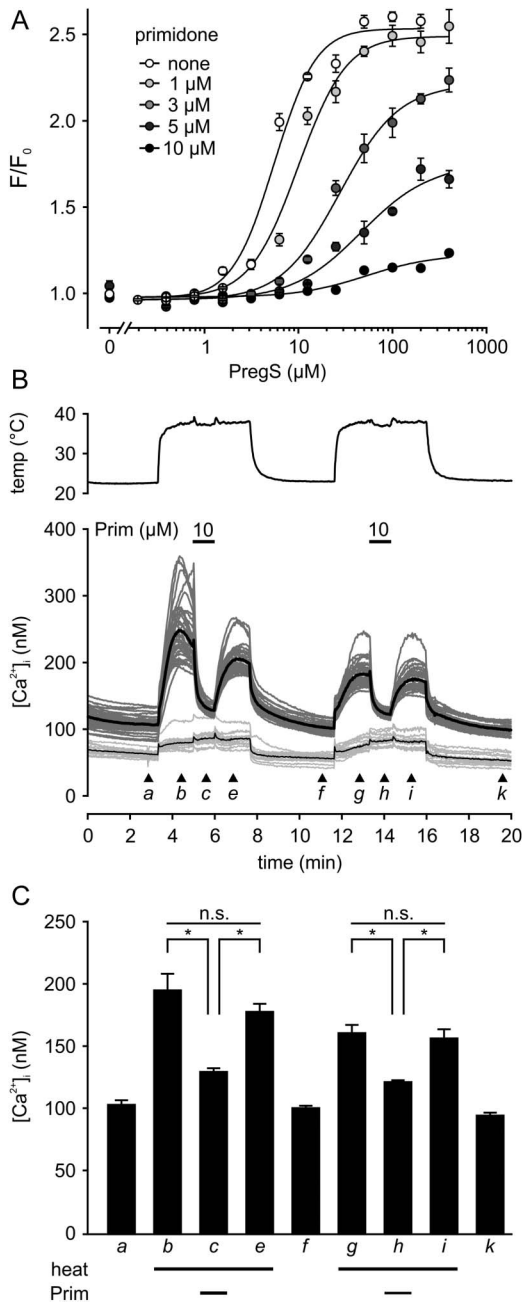


**Figure 6.** Primidone acts as an inhibitory allosteric modulator and prevents heat-induced activation of TRPM3. (A) Representative experiment of concentration-dependent pregnenolone sulfate (PregS)-induced Ca<sup>2+</sup> entry in stably transfected murine HEK<sub>TRPM3</sub> cells in the absence of primidone (open circles) and after incubation with different concentrations of primidone (1–10  $\mu\text{M}$ , filled circles) for 60 seconds ( $n = 3$  independent experiments in total). The left-most point per condition depicts controls without pregnenolone sulfate but primidone treatment. Data show mean values of quadruplets  $\pm$  SEM. EC<sub>50</sub> values (in  $\mu\text{M}$ ) were obtained by fitting a 4-parameter Hill equation to experimental data. (B) Primidone inhibits heat activation of TRPM3 channels. Representative single-cell [Ca<sup>2+</sup>]<sub>i</sub> imaging in HEK<sub>m</sub>TRPM<sub>3</sub>. Parental HEK293 cells served as control. The upper graph depicts the temperature profile throughout the experiment. The lower graph shows changes in [Ca<sup>2+</sup>]<sub>i</sub> in individual HEK<sub>m</sub>TRPM<sub>3</sub> cells (dark gray lines,  $n = 37$ ) or in parental HEK293 cells (light gray,  $n = 15$ ). The corresponding averages are given as black lines. Horizontal bars indicate the application of primidone (10  $\mu\text{M}$ ). Time points taken for analysis are marked (a–k). (C) Statistical analysis of heat-induced [Ca<sup>2+</sup>]<sub>i</sub> signals in HEK<sub>m</sub>TRPM<sub>3</sub> cells determined as illustrated in (B). Bars indicate mean values  $\pm$  SEM of 6 experiments. \* $P < 0.05$  heat vs heat plus primidone.

**Table 1**  
Impact of primidone on EC<sub>50</sub>, E<sub>max</sub>, and cooperativity of pregnenolone sulfate to induce Ca<sup>2+</sup> responses in HEK<sub>m</sub>TRPM<sub>3</sub> cells.

Primidone, $\mu\text{M}$	EC <sub>50</sub> , $\mu\text{M}$	E <sub>max</sub> (maximal F/F <sub>0</sub> )	Hill coefficient (n)
0	5.53	2.53	2.31
1	9.94	2.49	1.91
3	27.6	2.20	1.51
5	46.5	1.74	1.27
10	52.6	1.22	1.28

Pharmacodynamic parameters were calculated from data of fluorometric analyses of Ca<sup>2+</sup> entry in Fluo-4-loaded HEK<sub>m</sub>TRPM<sub>3</sub> cells as shown in Figure 6A by fitting a 4-parameter logistic function to the experimental data. EC<sub>50</sub> refers to the half maximally effective concentration of PregS.

duration per single response ( $P < 0.05$  both, 2-tailed unpaired Student  $t$  test, data not shown). This may suggest that behaviour in response to the block of chemical TRPM3 activation at doses higher than 5 mg·kg<sup>-1</sup> might be influenced secondarily by supraspinal effects of the active metabolites phenobarbital or phenylethylmalonamide.<sup>5,36</sup>

It has previously been shown that TRPM3 is also involved in the perception of noxious heat and inflammation-induced heat hyperalgesia in vivo, whereas cold hyperalgesia was not affected.<sup>33</sup> Consistently, primidone at doses of 0.5 and 2

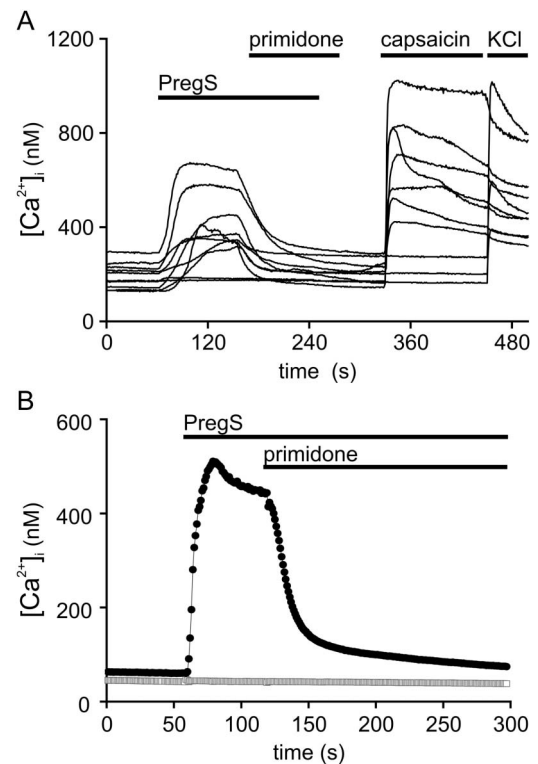


**Figure 7.** Primidone abrogates the pregnenolone sulfate (PregS)-induced increase in [Ca<sup>2+</sup>]<sub>i</sub> in freshly isolated rat DRG neurones and in transiently transfected HEK293 cells expressing human TRPM3. (A) Example traces of intracellular calcium concentrations of single, freshly isolated rat DRG neurones, during application of PregS (35  $\mu\text{M}$ ) and primidone (25  $\mu\text{M}$ ) as well as of the TRPV1 activator capsaicin (2  $\mu\text{M}$ ) and KCl (10 mM) to select neuronal cells that express voltage-gated potassium channels. (B) Fluorescent measurements in HEK293 cells expressing human TRPM3<sub>α2</sub> (black circles) or in nontransfected control cells (open circles). Pregnenolone sulfate (35  $\mu\text{M}$ ) and primidone (25  $\mu\text{M}$ ) were added as indicated by the horizontal bars.



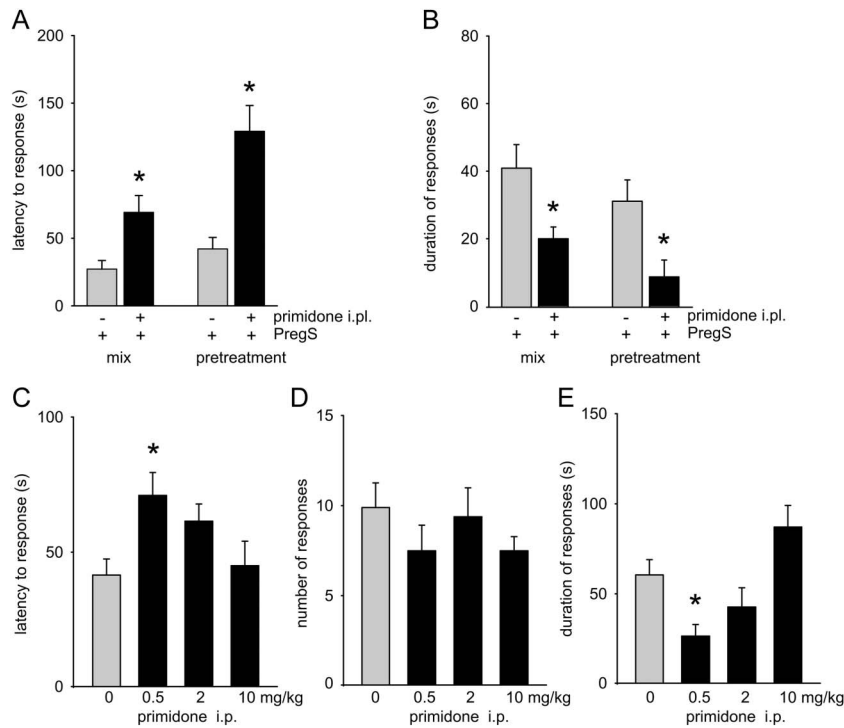


**Figure 8.** Nociceptive response to chemical pain induced by pregnenolone sulfate (PregS) in mice is inhibited by primidone. Latency (A) and duration of nociceptive responses (B) to PregS (5 nmol) (licking, lifting, and shaking) injected into the right hind paw either as a mixture with primidone (10 nmol) or 5 minutes after pretreatment with primidone. Data are presented as mean values  $\pm$  SEM ( $n = 12$  each). \* $P < 0.05$  vs vehicle group. Latency (C), number of responses (D), and total duration of nociceptive responses (E) to PregS (5 nmol, i.p.) were registered after intraperitoneal pretreatment with indicated doses of primidone. Data are presented as mean values  $\pm$  SEM ( $n = 8$  each). \* $P < 0.05$  vs vehicle group.

mg·kg<sup>-1</sup> (i.p.) prolonged the response latency (Fig. 9A) to the noxious thermal stimulus on the hot plate (52°C), whereas the latency at 10 mg·kg<sup>-1</sup> primidone did not differ from controls, similar to what was found in the PregS experiments, which argues for the strong dose dependency of the observed effects.

The exposure of the same animals to a novelty stimulating motor exploratory activity 15 minutes after administration of various doses of primidone (not shown) did not provide indication for interference of peripheral nociception with sedative central effects of primidone metabolites. In a second session, after 120 minutes, only the highest dose of 10 mg·kg<sup>-1</sup> primidone induced a slight reduction of exploratory activity (Fig. 9B) presumably related to sufficient metabolism of primidone.<sup>13,17</sup> The effectiveness of primidone was verified in a second thermal pain paradigm, the tail immersion test. A mean effective dose of 1 mg·kg<sup>-1</sup> primidone (i.p.) prolonged the latency to tail withdrawal (Fig. 9C).

Complete Freund adjuvant is widely used to induce inflammation, accompanied by mechanical allodynia or thermal hyperalgesia.<sup>6</sup> Complete Freund adjuvant administered into mice hind paws caused inflammatory paw swelling within 24 hours by about 70% (SDC Table S1) and enhanced pain sensitivity to a heat stimulus, indicative of hyperalgesia compared with the vehicle-treated group. In line with the primidone effects on acute noxious heat responses, systemic pretreatment with the drug (1 mg·kg<sup>-1</sup>) prevented the signs of CFA-induced sensitization (Fig. 9D) suggesting a clinically relevant role for TRPM3 inhibition in treating inflammatory hyperalgesia.

#### 4. Discussion

Starting from the initial identification of PregS or nifedipine as TRPM3 activators, TRPM3 pharmacology has since made

significant progress in terms of developing potent activators, such as CIM0216,<sup>7</sup> inhibitory E3-loop-targeting antibodies,<sup>19</sup> but also by identification of small, more drug-like molecules that inhibit TRPM3. Of them, mefenamic acid,<sup>11</sup> progesterone and dihydrotestosterone,<sup>15</sup> voriconazole,<sup>35</sup> and diclofenac<sup>29</sup> are approved drugs, but inhibit TRPM3 only at concentrations that vastly exceed plasma concentrations that are reached in their cognate therapeutic fields. Other drug-like compounds, such as the flavonoids naringenin, hesperetin, eriodictyol, liquiritigenin, or isosakuranetin exhibited a higher potency and promising selectivity.<sup>27,28</sup> Isosakuranetin also blocks the marked inward currents and release of peptides from skin nerves induced by CIM0216, a recently developed TRPM3 superagonist.<sup>7</sup> In addition, isosakuranetin and hesperetin were successfully applicable in in vivo pharmacology experiments, outlining the antinociceptive potential of TRPM3 inhibition.<sup>28</sup> However, a short half time of these compounds, which is presumably due to rapid hepatic metabolism, strongly limits their applicability in long-term protocols in experimental therapies.

Embarking on a screen for other drug-like compounds that inhibit TRPM3 activity, we identified maprotiline and primidone as approved drugs that concentration dependently inhibits Ca<sup>2+</sup> signalling and ionic currents through TRPM3. Because related drugs that act on the same targets as diclofenac or maprotiline were not effectively inhibiting TRPM3 and because IC<sub>50</sub> values to inhibit TRPM3 did not match with those reported for their cognate primary target mechanisms, we conclude that the mode of action is independent from cyclooxygenase or monoamine reuptake inhibition, respectively. As a consequence, orally administered therapeutic doses of diclofenac or maprotiline are not expected to result in plasma concentrations that would suffice to strongly

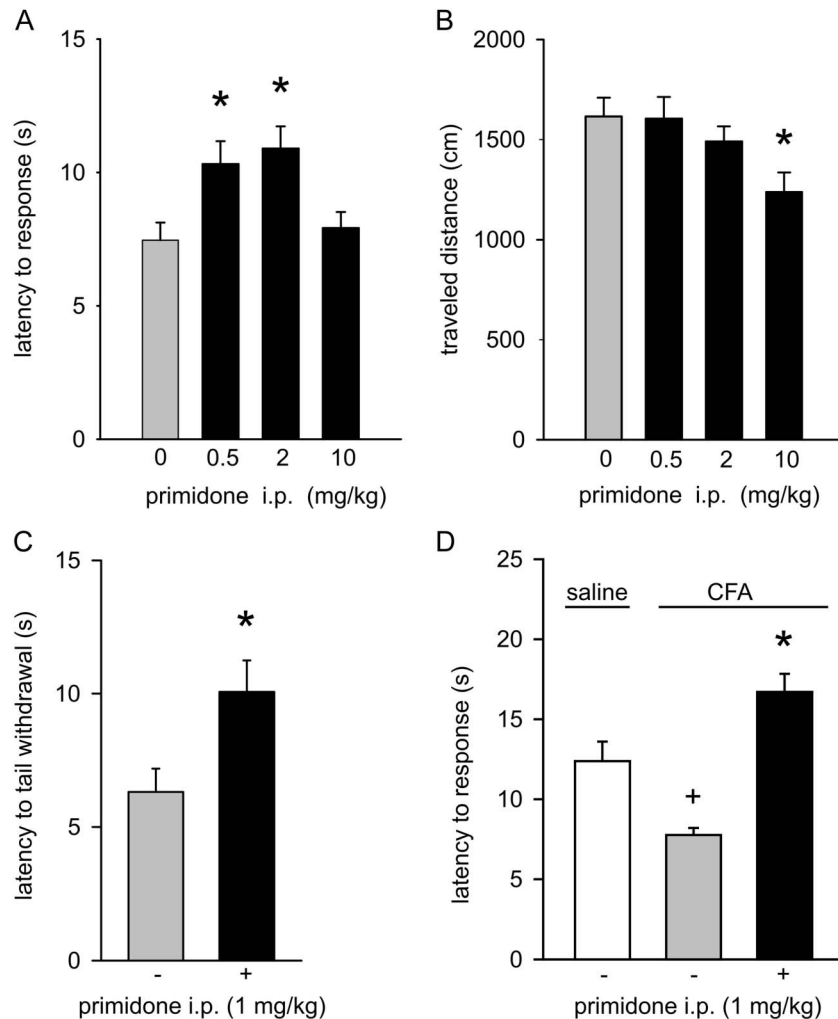


**Figure 9.** Systemically administered primidone attenuates nociceptive responses to noxious heat and thermal hyperalgesia in mice. (A) Effect of intraperitoneally administered primidone at indicated doses on the response latency of the hind paws on the hot plate (52°C). (B) Travelled distance of the same animals in an open field 120 minutes following drug administration (n = 10 each). (C) Effect of primidone (1 mg·kg<sup>-1</sup>, i.p.) on the response in the tail immersion test (48°C, n = 10 each). (D) Change in hot plate latency by treatment with primidone (1 mg·kg<sup>-1</sup>, i.p.) 24 hours after induction of thermal hyperalgesia by CFA injection into mice hind paws. Data are presented as mean values ± SEM (n = 8 each). \**P* < 0.05 vs vehicle (A–C) or vs CFA alone (D), +*P* < 0.05 vs vehicle group.

inhibit TRPM3 activity. This prediction is verified by IC<sub>50</sub> values for diclofenac found for recombinant human TRPM3 isoforms.<sup>29</sup> Because diclofenac is also topically applied in gels or solutions along with penetration-enhancing solvents such as DMSO or as epolamine salt,<sup>1</sup> it remains to be clarified whether part of its analgesic activity may be attributed to TRPM3 inhibition.

Because of its high selectivity and potency, and considering that therapeutic plasma concentrations of primidone clearly exceed the IC<sub>50</sub> of TRPM3 inhibition, primidone was the most interesting candidate and, therefore, characterised in more detail. In heterologously TRPM3-expressing cells, inhibition of TRPM3 currents was voltage independent, fast, reversible, and repeatable. A detailed analysis of concentration–response relationships indicated that primidone presumably acts as an inhibitory allosteric modulator with respect to the PregS binding site. Furthermore, primidone affects ion currents through the omega pore, which is thought to contribute to exacerbation of TRPM3-mediated pain.<sup>32</sup> In addition to abrogation of chemically evoked responses, heat-induced Ca<sup>2+</sup> entry through murine TRPM3 was reversibly inhibited by primidone. By blocking various modes of TRPM3 activation, primidone is expected to exert biological

activity toward pain perception via native TRPM3 channels. Similarly, in isolated rat DRG neurones, [Ca<sup>2+</sup>]<sub>i</sub> signals evoked by PregS were suppressed by primidone. Consistent with these data, in vivo experiments demonstrated the biological activity of primidone to counteract PregS- and noxious heat-induced nociceptive behaviour and to attenuate inflammatory thermal hyperalgesia, thus, mimicking the recently described phenotype of TRPM3-deficient transgenic mice.<sup>33</sup>

The recommended therapeutic plasma concentration of primidone is reported to range between 23 and 46 μM, giving rise to a plasma concentration of its major active metabolite phenobarbital of 15 to 40 μM.<sup>4,20,25</sup> With a plasma protein binding of less than 10%, a relative distribution volume of 0.6 L·kg<sup>-1</sup>, and an unrestricted partitioning into saliva, tears, or cerebrospinal fluid, pharmacokinetic data of primidone indicate an unrestricted penetration through biological membranes and into tissues. Thus, considering its IC<sub>50</sub> of about 0.6 μM and its effectivity toward human TRPM3, an almost complete inhibition of TRPM3 is presumably achieved during therapeutic application of the anticonvulsant. This as yet unrecognized effect of primidone has not caused adverse drug effects in cells or tissues that strongly

express TRPM3 and that can be directly attributed to the inhibition of this cation channel. Thus, inhibition of TRPM3 seems to be tolerable in humans. Of note, an expression of TRPM3 in insulin-secreting beta cells of pancreatic Langerhans islets has been reported, and TRPM3 activation can enhance insulin release *in vitro*.<sup>7,34</sup> Thus, TRPM3 inhibition by primidone might interfere with insulin levels and glucose homeostasis. Because, to the best of our knowledge, such effects have not yet been reported during more than 60 years of clinical experience with this drug, it may be questioned whether TRPM3 is a major determinant in regulating insulin secretion and blood glucose concentration in humans. This is in line with findings obtained in TRPM3-deficient transgenic mice, in which basal glucose concentrations do not differ from those in their wild-type littermates.<sup>33</sup>

In future, the availability of an approved drug which inhibits TRPM3 at therapeutic doses may be exploited to assess physiological and pathophysiological functions of this cation channel *in vivo* and across species, including humans. Moreover, the involvement of TRPM3 in diseased states may be tested using this drug. Although a pain-alleviating biological activity of TRPM3 inhibitors may be envisaged, evidence for an effective antinociceptive effect of TRPM3 inhibition in humans still needs to be shown. Applying the approved drug primidone at doses that are lower than those applied to treat convulsive disorders, the role of TRPM3 in mediating thermal pain or inflammatory hyperalgesia can be assessed. Finally, primidone may serve as a starting point for chemical modification to prevent a conversion to GABA<sub>A</sub> receptor-activating metabolites, and, thereby, to into a mono-mechanistic, TRPM3-selective drug.

### Conflict of interest statement

The authors have no conflicts of interest to declare.

Supported by the Deutsche Forschungsgemeinschaft (TRR 152 to M. Schaefer) and the Sino German Center (GZ1236 to U. Krügel).

### Acknowledgements

The authors thank Helga Sobottka, Marion Leonhardt, and Anne-Kathrin Krause for their expert technical assistance. The authors are grateful to Christian Harteneck (†), Tübingen, for providing the human TRPM3 cDNA. U. Krügel and I. Straub contributed equally to this work.

### Appendix A. Supplemental Digital Content

Supplemental Digital Content associated with this article can be found online at <http://links.lww.com/PAIN/A386>.

#### Article history:

Received 28 July 2016

Received in revised form 7 December 2016

Accepted 4 January 2017

Available online 12 January 2017

### References

- [1] Altman R, Bosch B, Brune K, Patrignani P, Young C. Advances in NSAID development: evolution of diclofenac products using pharmaceutical technology. *Drugs* 2015;75:859–77.
- [2] Alvin J, Goh E, Bush MT. Study of the hepatic metabolism of primidone by improved methodology. *J Pharmacol Exp Ther* 1975;194:117–25.
- [3] Bootman MD, Rietdorf K, Collins T, Walker S, Sanderson M. Ca<sup>2+</sup>-Sensitive fluorescent dyes and intracellular Ca<sup>2+</sup> imaging. In: Parys JB, Bootman M, Yule DI, Bultynck G, editors. *Calcium techniques*. Cold Spring Harbor: A Laboratory Manual Cold Spring Harbor Laboratory Press, 2014. p. 25–41.
- [4] Budakova L, Brozmanova H, Grundmann M, Fischer J. Simultaneous determination of antiepileptic drugs and their two active metabolites by HPLC. *J Sep Sci* 2008;31:1–8.
- [5] Carmody J, Knodler L, Murray S. Paradoxical modulation of nociception in mice by barbiturate agonism and antagonism: is a GABA site involved in nociception? *Eur J Neurosci* 1991;3:833–8.
- [6] Chillingworth NL, Donaldson LF. Characterisation of a Freund's complete adjuvant-induced model of chronic arthritis in mice. *J Neurosci Methods* 2003;128:45–52.
- [7] Held K, Kichko T, De CK, Klaassen H, Van BR, Vanherck JC, Marchand A, Reeh PW, Chaltin P, Voets T, Vriens J. Activation of TRPM3 by a potent synthetic ligand reveals a role in peptide release. *Proc Natl Acad Sci U S A* 2015;112:E1363–72.
- [8] Hellwig N, Plant TD, Janson W, Schafer M, Schultz G, Schaefer M. TRPV1 acts as proton channel to induce acidification in nociceptive neurons. *J Biol Chem* 2004;279:34553–61.
- [9] Hu H, Tian J, Zhu Y, Wang C, Xiao R, Herz JM, Wood JD, Zhu MX. Activation of TRPA1 channels by fenamate nonsteroidal anti-inflammatory drugs. *Pflugers Arch* 2010;459:579–92.
- [10] Kilkenny C, Browne WJ, Cuthill IC, Emerson M, Altman DG. Improving bioscience research reporting: the ARRIVE guidelines for reporting animal research. *J Pharmacol Pharmacother* 2010;1:94–9.
- [11] Klose C, Straub I, Riehle M, Ranta F, Krautwurst D, Ullrich S, Meyerhof W, Harteneck C. Fenamates as TRP channel blockers: mefenamic acid selectively blocks TRPM3. *Br J Pharmacol* 2011;162:1757–69.
- [12] Latorre R, Zaelzer C, Brauchi S. Structure-functional intimacies of transient receptor potential channels. *Q Rev Biophys* 2009;42:201–46.
- [13] Leal KW, Rapport RL, Wilensky AJ, Friel PN. Single-dose pharmacokinetics and anticonvulsant efficacy of primidone in mice. *Ann Neurol* 1979;5:470–4.
- [14] Liao M, Cao E, Julius D, Cheng Y. Structure of the TRPV1 ion channel determined by electron cryo-microscopy. *Nature* 2013;504:107–12.
- [15] Majeed Y, Tumova S, Green BL, Seymour VA, Woods DM, Agarwal AK, Naylor J, Jiang S, Picton HM, Porter KE, O'Regan DJ, Muraki K, Fishwick CW, Beech DJ. Pregnenolone sulphate-independent inhibition of TRPM3 channels by progesterone. *Cell Calcium* 2012;51:1–11.
- [16] McGrath JC, Drummond GB, McLachlan EM, Kilkenny C, Wainwright CL. Guidelines for reporting experiments involving animals: the ARRIVE guidelines. *Br J Pharmacol* 2010;160:1573–6.
- [17] Middaugh LD, Blackwell LA, Boggan WO, Zemp JW. Brain concentrations of phenobarbital and behavioral activation or depression. *Pharmacol Biochem Behav* 1981;15:723–8.
- [18] Moiseenkova-Bell VY, Wensel TG. Hot on the trail of TRP channel structure. *J Gen Physiol* 2009;133:239–44.
- [19] Naylor J, Milligan CJ, Zeng F, Jones C, Beech DJ. Production of a specific extracellular inhibitor of TRPM3 channels. *Br J Pharmacol* 2008;155:567–73.
- [20] Neels HM, Sierens AC, Naelaerts K, Scharpe SL, Hatfield GM, Lambert WE. Therapeutic drug monitoring of old and newer anti-epileptic drugs. *Clin Chem Lab Med* 2004;42:1228–55.
- [21] NIH. Guide for the care and use of laboratory animals. Bethesda: National Institutes of Health, Public Health Service, 1986.
- [22] Nörenberg W, Sobottka H, Hempel C, Plötz T, Fischer W, Schmalzing G, Schaefer M. Positive allosteric modulation by ivermectin of human but not murine P2X7 receptors. *Br J Pharmacol* 2012;167:48–66.
- [23] Oberwinkler J, Lis A, Giehl KM, Flockerzi V, Philipp SE. Alternative splicing switches the divalent cation selectivity of TRPM3 channels. *J Biol Chem* 2005;280:22540–8.
- [24] Oliver AE, Baker GA, Fugate RD, Tablin F, Crowe JH. Effects of temperature on calcium-sensitive fluorescent probes. *Biophys J* 2000;78:2116–26.
- [25] Patsalos PN, Berry DJ. Therapeutic drug monitoring of antiepileptic drugs by use of saliva. *Ther Drug Monit* 2013;35:4–29.
- [26] Paulsen CE, Armache JP, Gao Y, Cheng Y, Julius D. Structure of the TRPA1 ion channel suggests regulatory mechanisms. *Nature* 2015;520:511–17.
- [27] Straub I, Krügel U, Mohr F, Teichert J, Rizun O, Konrad M, Oberwinkler J, Schaefer M. Flavanones that selectively inhibit TRPM3 attenuate thermal nociception *in vivo*. *Mol Pharmacol* 2013;84:736–50.
- [28] Straub I, Mohr F, Stab J, Konrad M, Philipp S, Oberwinkler J, Schaefer M. Citrus fruit and fabacea secondary metabolites potently and selectively block TRPM3. *Br J Pharmacol* 2013;168:1835–50.
- [29] Suzuki H, Sasaki E, Nakagawa A, Muraki Y, Hatano N, Muraki K. Diclofenac, a nonsteroidal anti-inflammatory drug, is an antagonist of human TRPM3 isoforms. *Pharmacol Res Perspect* 2016;4:1–14.
- [30] Ueda H, Inoue M, Yoshida A, Mizuno K, Yamamoto H, Maruo J, Matsuno K, Mita S. Metabotropic neurosteroid/sigma-receptor

- involved in stimulation of nociceptor endings of mice. *J Pharmacol Exp Ther* 2001;298:703–10.
- [31] Urban N, Hill K, Wang L, Kuebler WM, Schaefer M. Novel pharmacological TRPC inhibitors block hypoxia-induced vasoconstriction. *Cell Calcium* 2012;51:194–206.
- [32] Vriens J, Held K, Janssens A, Toth BI, Kerselaers S, Nilius B, Vennekens R, Voets T. Opening of an alternative ion permeation pathway in a nociceptor TRP channel. *Nat Chem Biol* 2014;10:188–95.
- [33] Vriens J, Owsianik G, Hofmann T, Philipp SE, Stab J, Chen X, Benoit M, Xue F, Janssens A, Kerselaers S, Oberwinkler J, Vennekens R, Gudermann T, Nilius B, Voets T. TRPM3 is a nociceptor channel involved in the detection of noxious heat. *Neuron* 2011;70:482–94.
- [34] Wagner TF, Loch S, Lambert S, Straub I, Mannebach S, Mathar I, Dufer M, Lis A, Flockerzi V, Philipp SE, Oberwinkler J. Transient receptor potential M3 channels are ionotropic steroid receptors in pancreatic beta cells. *Nat Cell Biol* 2008;10:1421–30.
- [35] Xiong WH, Brown RL, Reed B, Burke NS, Duvoisin RM, Morgans CW. Voriconazole, an antifungal triazol that causes visual side effects, is an inhibitor of TRPM1 and TRPM3 channels. *Invest Ophthalmol Vis Sci* 2015; 56:1367–73.
- [36] Yokoro CM, Pesquero SM, Turchetti-Maia RM, Francischi JN, Tatsuo MA. Acute phenobarbital administration induces hyperalgesia: pharmacological evidence for the involvement of supraspinal GABA-A receptors. *Braz J Med Biol Res* 2001;34:397–405.